Original Article

Different hydration protocols for the quantification of healthy tissue uptake of half-dose ^{18}F-FDG total-body positron emission tomography–computed tomography: a prospective study

Yanyan Cao[1,2,3], Danjie Cai[1,2,3], Xiuli Sui[1,2,3], Xiangqing Wang[1,2,3], Jun Song[1,2,3], Hui Tan[1,2,3], Pengcheng Hu[1,2,3], Yiqiu Zhang[1,2,3], Haojun Yu[1,2,3], Hongcheng Shi[1,2,3]

[1]Shanghai Institute of Medical Imaging, Shanghai, China; [2]Department of Nuclear Medicine, Zhongshan Hospital, Fudan University, Shanghai, China; [3]Institute of Nuclear Medicine, Fudan University, Shanghai, China

Contributions: (I) Conception and design: H Shi, Y Cao; (II) Administrative support: H Shi, P Hu, Y Zhang; (III) Provision of study materials or patients: X Wang, J Song, H Yu; (IV) Collection and assembly of data: Y Cao, D Cai, X Sui; (V) Data analysis and interpretation: Y Cao, D Cai, H Tan; (VI) Manuscript writing: All authors; (VII) Final approval of manuscript: All authors.

Correspondence to: Hongcheng Shi, MD, PhD. Shanghai Institute of Medical Imaging, Shanghai, China; Department of Nuclear Medicine, Zhongshan Hospital, Fudan University, No. 180 in Fenglin Road, Shanghai 200032, China; Institute of Nuclear Medicine, Fudan University, Shanghai, China. Email: shi.hongcheng@zs-hospital.sh.cn.

Background: This study aimed to investigate the effects of the volume and time of hydration on the quantification of healthy tissue uptake for 2-deoxy-2-[^{18}F]-fluoro-D-glucose (^{18}F-FDG) total-body positron emission tomography (PET)–computed tomography (CT) with half-dose activity.

Methods: This study prospectively enrolled 180 patients who underwent a total-body PET-CT scan 10 min after injection of a half-dose (1.85 MBq/kg) of ^{18}F-FDG. These patients were placed in hydration groups (30 patients in each group) according to different hydration volumes and times: oral hydration with 500 mL of water 20 min before (G1), 5 min after (G2), and 30 min after (G3) the ^{18}F-FDG injection; and oral hydration with 200 mL of water 20 min before (G4), 5 min after (G5), and 30 min after (G6) the ^{18}F-FDG injection. Another 30 patients underwent dynamic imaging without hydration and were used a nonhydration group. The analysis of quantification of healthy tissue uptake included the maximum standardized uptake value (SUVmax) and the mean SUV (SUVmean) of the blood pool and muscle, as well as the SUVmax, SUVmean, and signal-to-noise ratio (SNR) of the liver.

Results: The SUVmax of the blood pool (2.33±0.36), liver (3.03±0.42), and muscle (0.81±0.15) was significantly higher in the nonhydration group than in any of the 6 hydrated groups ($P<0.05$ for all hydration groups *vs*. nonhydration group). Muscle SUVmax and SUVmean were significantly ($P<0.05$) lower in G1 and G2 than in G3 and were lower in G4 and G5 than in G6. The SUVmax and SUVmean of the blood pool were significantly ($P<0.05$) lower in G1 than in G3 and G4 and lower in G3 than in G6.

Conclusions: When total-body PET-CT with a half dose of ^{18}F-FDG activity is performed, hydration can significantly affect the quantification of healthy tissue uptake. Oral administration of 500 mL of water 20 min before injection could reduce background radioactivity.

Keywords: Hydration protocols; quantification; total-body positron emission tomography–computed tomography (total-body PET-CT); half-dose; 2-deoxy-2-[^{18}F]-fluoro-D-glucose (^{18}F-FDG)

Submitted May 03, 2022. Accepted for publication Jun 16, 2023. Published online Jul 21, 2023.
doi: 10.21037/qims-22-440
View this article at: https://dx.doi.org/10.21037/qims-22-440

Introduction

2-deoxy-2-^{18}F-fluoro-D-glucose positron emission tomography–computed tomography (^{18}F-FDG PET-CT) has an important role in the tumor detection, staging, restaging, and assessment of therapeutic response (1-4) and is widely used in clinical practice. ^{18}F-FDG is an analog of glucose, with the degree of FDG uptake representing the metabolic activity of cells (5). Unlike glucose, which is completely reabsorbed in the proximal tubules of the kidney, ^{18}F-FDG is excreted by the kidneys into the urine and accumulates in the urinary tract (6).

Hydration is important to reducing tracer uptake in normal tissue and for radiation safety reasons [i.e., "as low as reasonably achievable" (ALARA)], as is emphasized in the relevant guidelines (7-9). However, these guidelines are inconsistent in terms of hydration time and fluid volume. The European Association of Nuclear Medicine guidelines recommends 1 L of water 2 h before injection and another 0.5 L during the uptake period if it can be tolerated (7). The National Cancer Institute recommends that patients consume at least 2–3 glasses of water (12 ounces or 355 mL per glass) during fasting and another 250–500 mL of water after injection and before scanning (8). The American College of Radiology suggests oral hydration or intravenous administration in special circumstances. Finally, The Society of Nuclear Medicine and Molecular Imaging simply mentions oral hydration with water but does not go into greater detail (9). In clinical practice, the hydration protocols implemented also differ from one healthcare institution to another, and there is no relevant evidence clarifying the degree to which hydration protocols effect the quantification of healthy tissue uptake.

Total-body PET-CT with a long axial field of view (FOV) (10), ultrahigh system sensitivity, and good spatial resolution has been used clinically and become a new research focus (11,12), with superior image quality and a lower dose of radioactivity being new research trends (13-18). Compared to conventional PET-CT, total-body PET-CT can detect subtle differences in coincidence photon counts between tissues (19,20) and acquires the whole-body image in a one-bed position, which eliminates the influence of overlap and other factors during multibed positioning, thus providing a more objective evaluation on the quantification of tissue uptake (21). Therefore, this study was aimed at identifying the optimal hydration procedure for total-body PET-CT and providing supporting evidence for optimizing hydration protocols.

Methods

Patients

This study was conducted in accordance with the Declaration of Helsinki (as revised in 2013) and was approved by the Ethics Committee of Zhongshan Hospital, Fudan University (No. B2019-160R). Written informed consent was obtained from all enrolled patients before the study began. In all, 332 patients who underwent static imaging with different hydration protocols and another 42 patients who underwent dynamic imaging without hydration were prospectively enrolled. PET-CT scans were performed with a half-dose of ^{18}F-FDG activity (1.85 MBq/kg) using the uEXPLORER (United Imaging Healthcare, Shanghai, China). All scans were performed and analyzed at Zhongshan Hospital, Fudan University, from January 2020 to September 2022. The inclusion criteria were as follows: (I) age 18 to 80 years, (II) no diabetes and a fasting blood glucose level <7.8 mmol/L, (III) normal renal function, and (IV) acceptable clinical conditions and good compliance. Meanwhile, the exclusion criteria were as follows: (I) excessive tumor load (diameter of tumor >10 cm or more than 5 metastases) or high bone marrow uptake (defined visually as intense bone marrow uptake higher than the liver), (II) obstructive pathology of the urinary tract, (III) moderate-to-severe fatty liver or cirrhosis, (IV) cancer patients with a history of radiotherapy or chemotherapy, (V) drinking water during the 6-hour fasting period, and (VI) ^{18}F-FDG injection infiltration. Ultimately, 180 participants with static imaging and 30 with dynamic imaging were eventually included.

As shown in *Figure 1*, patients were randomized divided into 6 groups according to hydration volume and time: oral hydration with 500 mL of water 20 min before (G1), 5 min after (G2), and 30 min after (G3) the ^{18}F-FDG injection; and oral hydration with 200 mL of water 20 min before (G4), 5 min after (G5), and 30 min after (G6) the ^{18}F-FDG injection. Another 30 patients underwent dynamic PET-CT without hydration and were included in the nonhydration control group.

PET-CT examination

Patients fasted for at least 6 h before the ^{18}F-FDG injection, and blood glucose levels were measured before injection. Then, ^{18}F-FDG (1.85 MBq/kg) was injected. The 6 hydration groups, totaling 180 patients, underwent static PET-CT after resting quietly for about 60 min after the injection of ^{18}F-FDG, with an acquisition time of 10 min. Patients were allowed to urinate at any time

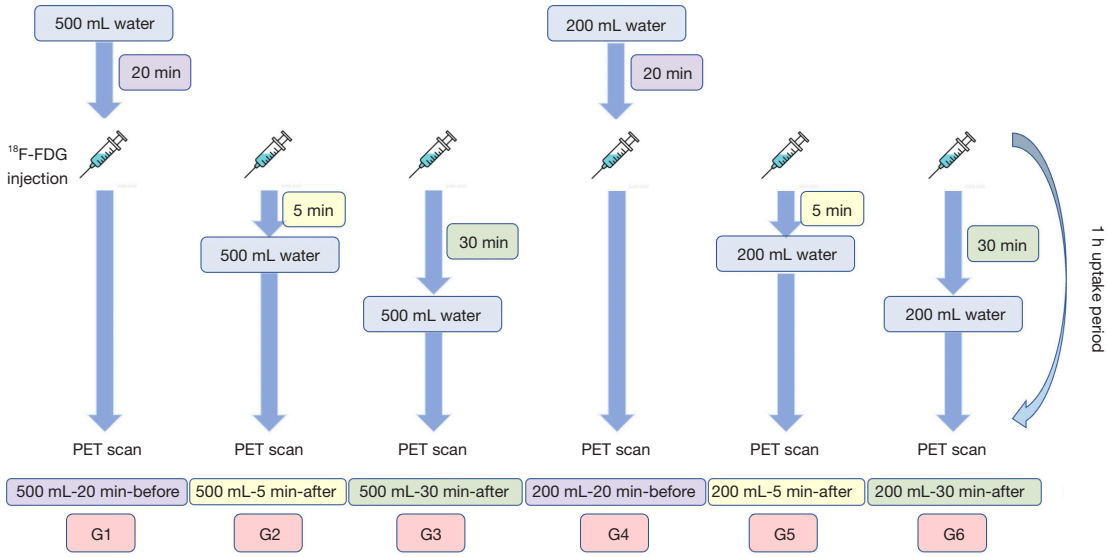

Figure 1 Overview of the 6 different preparation protocols. Oral hydration with 500 mL of water 20 min before (500 mL-20 min-before, G1), 5 min after (500 mL-5 min-after, G2), and 30 min after (500 mL-30 min-after, G3) the ^{18}F-FDG injection; and oral hydration with 200 mL of water 20 min before (200 mL-20 min-before, G4), 5 min after (200 mL-5 min-after, G5), and 30 min after (200 mL-30 min-after, G6) the ^{18}F-FDG injection. ^{18}F-FDG, 2-deoxy-2-[^{18}F]-fluoro-D-glucose; PET, positron emission tomography.

during the ^{18}F-FDG uptake phase and were instructed to empty their bladder before PET-CT image acquisition. The nonhydration control group included 30 patients who underwent a dynamic study with total-body PET-CT after injection. The PET reconstruction parameters were as follows: ordered subset expectation maximization (OSEM) to reconstruct PET images with time-of-flight (TOF) and point spread function (PSF) modeling, 3 iterations and 20 subsets, a 192×192 matrix, at thickness of 1.443 mm, Gaussian postfilter (3 mm), and all necessary corrections. The CT scan parameters were as follows: tube voltage, 120 kV; tube current, 140 mA; pitch, 1.0; collimation, 0.5 mm; and reconstructed slice thickness, 0.5 mm. The acquisition time of dynamic PET was 75 min for 21 participants and 60 min for 9 participants. Dynamic PET images were constructed from the last 10 min of data to simulate static acquisition scenarios.

Analysis of PET images

The analysis of images was performed separately by 2 senior nuclear medicine physicians with over 5 years of interpreting PET-CT images (Hu, 11 years; Tan, 5 years). As shown in *Figure 2*, on the transverse section with the maximal diameter of the liver, four 2D circular regions of interest (ROIs) with a diameter of 20 mm were manually drawn in homogenous areas (1 on the left lobe and 3 on the right lobe), with lesions and major blood vessels being avoided. The maximum standard uptake value (SUVmax), mean standard uptake value (SUVmean), and standard deviation (SD) of the ROIs in the liver were recorded. The SUVmax, SUVmean, and SD of the liver were calculated as the averages of the 4 ROIs. The signal-to-noise ratio (SNR) of the liver was calculated by dividing the liver SUVmean in the ROI by the SD (22). Along the medial wall of the root of the aortic arch, an ROI was placed in the lumen to measure the SUVmax and SUVmean of the blood pool. The SUVmax and SUVmean of both sides of the gluteus maximus were measured at the transverse section with the third sacral foramen level by drawing ROIs with a diameter of 20 mm. A circular ROI with a diameter of 10 mm was delineated on the maximum coronal section of both kidneys to measure the SUVmax of the renal parenchyma. The 3D volume of interest (VOI) was delineated in the bladder cavity, and the SUVmax was recorded. The PET parameters of the gluteus maximus and kidney were calculated as the average of both sides. The values reported by each observer were averaged for intergroup comparison.

Statistical analysis

Quantitative data following normal distribution are

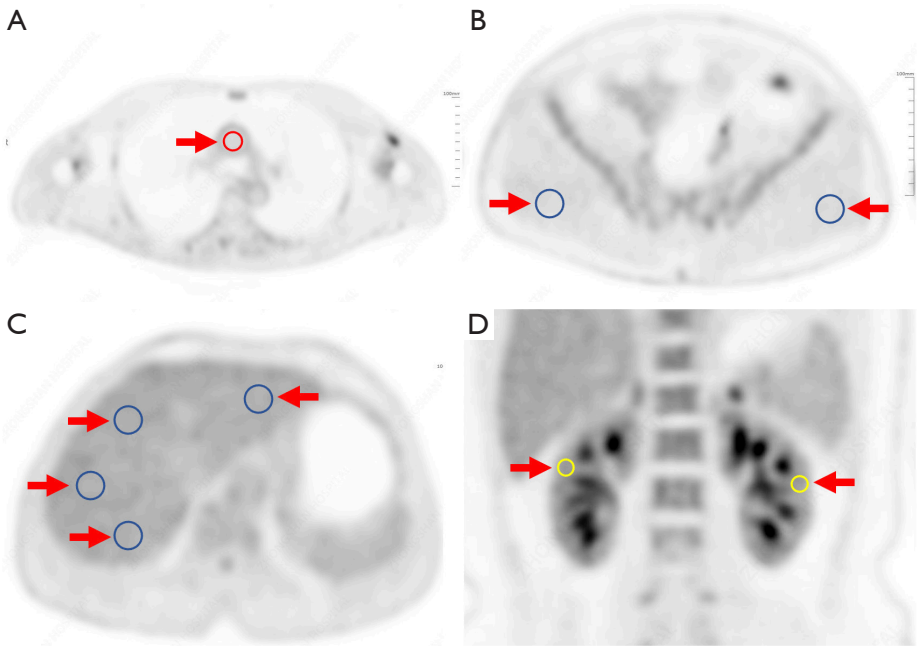

Figure 2 The placement of the standard ROI for normal tissues (arrowed circles). (A) A blood pool along the medial wall of the root of the aortic arch; the ROI was placed in the lumen. (B) Muscle: ROIs with a diameter of 20 mm were placed at the transverse section with the third sacral foramen level. (C) Liver: four 2D circular ROIs with a diameter of 20 mm were placed in homogenous areas (1 on the left lobe and 3 on the right lobe) on the transverse section with the maximal diameter of the liver, with lesions and major blood vessels being avoided. (D) Kidney: ROIs with a diameter of 10 mm were placed in the renal parenchyma on the maximum coronal section of both kidneys. ROI, region of interest.

expressed as the mean ± SD, while nonnormally distributed data are reported as the median (P75, P25) percentile. Qualitative data were compared using the chi-squared test. The Mann-Whitney test was used to compare the differences in PET parameters between the 500-mL and 200-mL groups at the same hydration time, and the Kruskal-Wallis rank-sum test and Dunn test were used to compare the differences in PET parameters between the 3 hydration time subgroups at the same water volume and the clinical quantitative information between the groups. SPSS software (version 20.0; IBM Corp., Armonk, NY, USA) and GraphPad Prism 8 (GraphPad Software Inc., San Diego, CA, USA) were used to perform statistical analysis, with P values <0.05 indicating a significant difference.

Results

Patients

A total of 332 participants were prospectively hydrated, and another 42 participants underwent dynamic PET. Of these, 164 were excluded due to failure to cooperate with the hydration protocol (n=27), failure to meet the ^{18}F-FDG uptake time (n=78), excessive tumor load (n=27), obstructive pathology of the urinary tract (n=7), moderate-to-severe fatty liver or cirrhosis (n=11), or ^{18}F-FDG injection infiltration (n=14). Finally, a total of 210 patients (men, 129; women, 81) with an average age of 56.7±12.4 years (range, 19–80 years) were enrolled. The clinical characteristics of the patients in the different groups are shown in *Table 1*, and details about the cancers are shown in *Table 2*. There was no statistical difference in the ^{18}F-FDG uptake time between the 7 groups. The age, sex, weight, height, body mass index (BMI), and blood glucose level were comparable between the 7 groups. All enrolled patients tolerated the hydration protocols well.

The quantitative parameters of the blood pool, muscle, liver, kidney, and bladder in the 6 hydration groups are summarized in *Table 3*.

Effect of water volume on the quantification of healthy tissue uptake

For hydration at 20 min before or 30 min after injection,

Table 1 Clinical characteristics of the participants in the 7 Groups (n=30 for all groups)

Characteristic	G1	G2	G3	G4	G5	G6	Nonhydration	P
Gender (male/female)	16/14	21/9	20/10	19/11	19/11	18/12	16/14	0.81
Age (years)	58.6±11.7	56.6±14.5	57.9±9.4	55.0±11.0	59.1±13.2	57.2±12.0	52.7±14.2	0.64
Weight (kg)	60.7±6.8	62.3±8.9	62.3±10.2	63.7±12.5	61.7±10.9	64.8±11.4	62.9±11.4	0.85
Height (cm)	164.8±5.7	166.3±5.9	166.0±7.2	166.0±8.3	164.2±8.8	166.3±9.1	165.0±8.3	0.97
BMI (kg/m^2)	22.3±2.5	22.5±2.3	22.5±3.2	23.0±3.1	22.8±3.2	23.1±3.5	23.0±3.4	0.80
Blood glucose (mmol/L)	5.5±0.6	5.4±0.8	5.4±0.6	5.3±0.5	5.3±0.7	5.2±0.6	5.6±0.8	0.23
Injected dose (MBq)	119.9±19.0	117.2±17.5	117.7±17.8	119.5±21.7	123.3±23.1	118.5±22.6	121.3±18.7	0.88
Uptake time (min)	64.1±8.4	64.1±9.7	64.3±9.4	60.4±9.9	61.8±8.8	60.4±9.3	60.5±7.0	0.22

Data are presented as the mean ± SD or the number of patients. BMI, body mass index; SD, standard deviation.

Table 2 Pathological distribution of the primary tumors and suspected metastases in the 7 groups (n=30 for all groups)

Pathological distribution	G1	G2	G3	G4	G5	G6	Nonhydration
Head and neck tumor (n=9)	2	2	1	2	1	0	1
Esophageal cancer† (n=17)	1	2	3	4	2	3	2
Lung cancer† (n=50)	6	7	7	9	9	8	4
Gastric cancer (n=28)	6	6	3	1	5	3	4
Breast cancer (n=8)	1	0	2	1	2	1	1
Liver cancer (n=8)	1	0	2	0	0	1	4
Colorectal cancer (n=33)	5	4	5	5	3	6	5
Gynecological tumor (n=7)	0	1	2	1	0	1	2
Other tumor (n=4)	0	1	0	0	0	2	1
No malignant lesions (n=46)	8	7	5	7	8	5	6
With liver metastases‡ (n=6)	1	1	0	2	0	0	2
Para-aortic node metastasis† (n=7)	2	1	1	2	0	1	0

†, the distance between the primary tumors and the region-of-interest placement location of the blood pool was more than 5 cm. The distance between the para-aortic node metastasis and the ROI placement location of the blood pool was more than 2 cm. ‡, the number of metastases lesions was less than 5 for any participant, and the diameter was less than 2 cm for any liver metastasis lesion. ROI, region of interest.

the SUVmax and SUVmean of the blood pool (*Figure 3*) in the 500-mL group were significantly lower than in the 200-mL group (P<0.05 for G1 *vs.* G4 and for G3 *vs.* G6). With hydration at 5 min after injection, the SUVmax and SUVmean of the blood pool were 1.74 and 1.55 in the 500-mL group (G2), and 1.85 and 1.66 in the 200-mL group (G5), respectively (P=0.06 for SUVmax and P=0.07 for SUVmean), with differences approaching the significance threshold. There was a tendency of a decreased SUVmax of the renal parenchymal and bladder cavity related to increased renal tracer excretion with a high volume of water, with a statistically significant difference in SUVmax of the bladder cavity between G1 and G4 (P<0.05). However, there were no significant differences in muscle SUVmax or SUVmean (*Figure 4*) or in liver SUVmax, SUVmean, SD, and SNR between the 500-mL group and the 200-mL group at any hydration time (P>0.05 for G1 *vs.* G4, G2 *vs.* G5, and G3 *vs.* G6) (*Figure 5A-5D*).

Effect of water administration time on the quantification of healthy tissue uptake

With the delay in hydration time, the SUVmax and SUVmean of the blood pool and muscle tended to increase.

Table 3 Quantitative parameters from the 6 hydration groups

Measurement	G1	G2	G3	G4	G5	G6	Nonhydration
Blood							
SUVmax	1.62±0.20†,‡	1.74±0.22	1.77±0.31§	1.80±0.28	1.85±0.23	1.93±0.26	2.33±0.36¶
SUVmean	1.44±0.23†,‡	1.55±0.19	1.60±0.28§	1.61±0.23	1.66±0.24	1.73±0.23	1.98±0.29¶
Muscle							
SUVmax	0.69±0.10‡	0.70±0.10‡	0.79±0.14	0.68±0.10§	0.70±0.10§	0.78±0.10	0.81±0.15$^{\#}$
SUVmean	0.58±0.12‡	0.58±0.12‡	0.68±0.14	0.57±0.10§	0.59±0.10§	0.68±0.11	0.62±0.13$^{\#}$
Liver							
SUVmax	2.55±0.39	2.58±0.36	2.61±0.50	2.61±0.39	2.55±0.40	2.70±0.32	3.03±0.42¶
SUVmean	2.29±0.35	2.31±0.32	2.34±0.45	2.35±0.34	2.27±0.38	2.43±0.28	2.73±0.37¶
SD	0.12±0.02	0.12±0.02	0.12±0.03	0.12±0.02	0.12±0.02	0.13±0.02	0.14±0.03¶
SNR	19.80±2.26	19.82±1.64	19.56±2.29	19.54±2.02	19.51±2.23	19.69±2.30	19.79±2.72
Kidney							
SUVmax	2.84±0.33	2.87±0.29	2.89±0.35	2.96±0.53	2.98±0.42	3.02±0.39	3.54±0.41¶
Bladder							
SUVmax	24.6† (101.5–12.5)	47.8 (114.7–19.1)	91.9 (140.7–19.1)	66.9 (180.2–23.7)	66.6 (153.9–30.5)	81.6 (190.6–26.9)	231.4¶ (85.6–377.1)

Data are presented as the mean ± SD or median (interquartile range). Difference between groups were significantly different if the P<0.05 after corrections. †, the mean SUV was significantly different from G4; ‡, the mean SUV was significantly different from G3; §, the SUV was significantly different from G6; ¶, the SUV or SD was significantly different from any of the hydration groups (G1–G6); $^{\#}$, the SUV was significantly different from any of G1 to G4. SUVmax, maximum standardized uptake value; SUVmean, mean standardized uptake value; SD, standard deviation; SNR, signal-to-noise ratio.

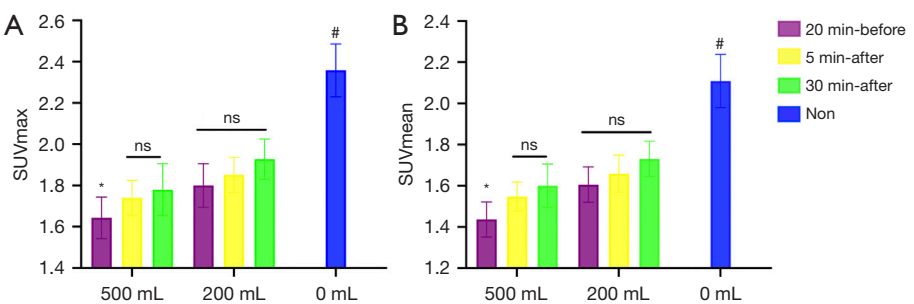

Figure 3 The quantitative parameters of the blood pool in the 7 groups. There was a significant difference in SUVmax and SUVmean of the blood pool between G1 and G4 or between G3 and G6 (P<0.05). The difference between G2 and G5 approached the threshold of significance (P=0.06). *, the SUVmax and SUVmean of G1 were significantly lower than those of G3. #, the SUVmax and SUVmean of the blood pool were significantly higher in the nonhydration group than in any hydration group (P<0.05). ns, no statistically significant difference. SUVmax, maximum standardized uptake value; SUVmean, mean standardized uptake value.

Specifically, with 500 mL of water, the SUVmax and SUVmean of the blood pool in G1 was significantly lower than in G3 (adjusted P<0.05). With 200 mL of water, the SUVmax of the blood pool was 1.80, 1.85, and 1.93 in G4, G5, and G6, respectively, with no significant difference (P>0.05). In addition, with 500 mL of water, the SUVmax and SUVmean of the muscle in G3 were significantly higher than in G1 and G2 (adjusted P<0.05 for G1 *vs.* G3 and for

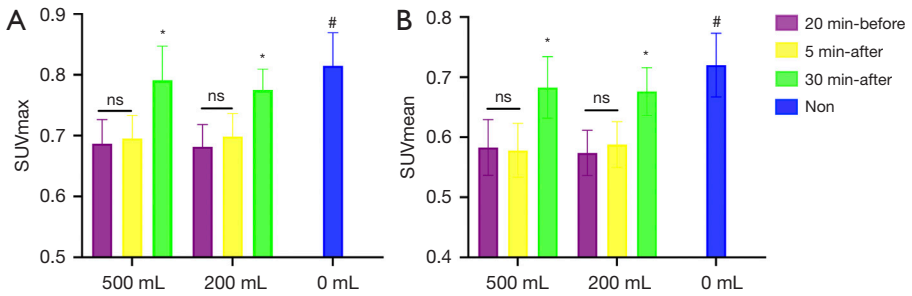

Figure 4 The quantitative parameters of the muscle in the 7 groups. There was no significant difference in SUVmax and SUVmean of the muscle between G1 and G4, between G2 and G5, or between G3 and G6 (P>0.05). *, SUVmax and SUVmean of the muscle were significantly higher in G3 than in G1 and G2 and higher in G6 than in G4 and G5 (P<0.05). #, the muscle SUVmax and SUVmean were significantly higher in the nonhydration group than in G1, G2, G4, and G5 (P<0.05). ns, no statistically significant difference. SUVmax, maximum standardized uptake value; SUVmean, mean standardized uptake value.

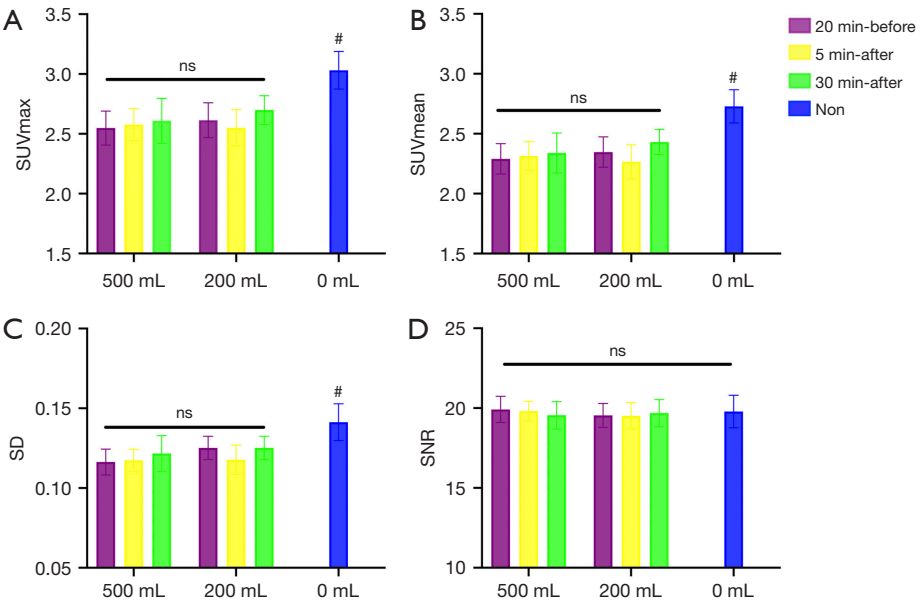

Figure 5 The quantitative parameters of the liver in the 7 groups. The liver SUVmax, SUVmean, and SD were compared among all 6 hydration groups, with all P>0.05. The liver SNR was compared among all the 7 groups, with all P>0.05. #, the liver SUVmax, SUVmean, and SD of the nonhydration group were significantly higher than those in all the hydration groups, with P<0.05 for all hydration groups *vs.* the nonhydration group. ns, no statistically significant difference. SUVmax, maximum standardized uptake value; SUVmean, mean standardized uptake value; SD, standard deviation; SNR, signal-to-noise ratio.

G2 *vs.* G3). Similarly, with 200 mL of water, the SUVmax and SUVmean of the muscle in G6 were significantly higher than in G4 and G5 (adjusted P<0.05 for G4 *vs.* G6 and for G5 *vs.* G6). There was no statistically significant difference in the liver SUVmax, SUVmean, SD, or SNR between G1, G2, and G3 or between G4, G5, and G6 (P>0.05 for G1, G2, *vs.* G3 and for G4, G5, *vs.* G6).

The quantification of healthy tissue uptake between the hydration groups and nonhydration group

The SUVmax (2.33±0.36) and SUVmean (1.98±0.29) of the blood pool in the nonhydration control group were significantly higher than in each of the 6 groups (P<0.05 for all hydration groups *vs.* nonhydration group). The

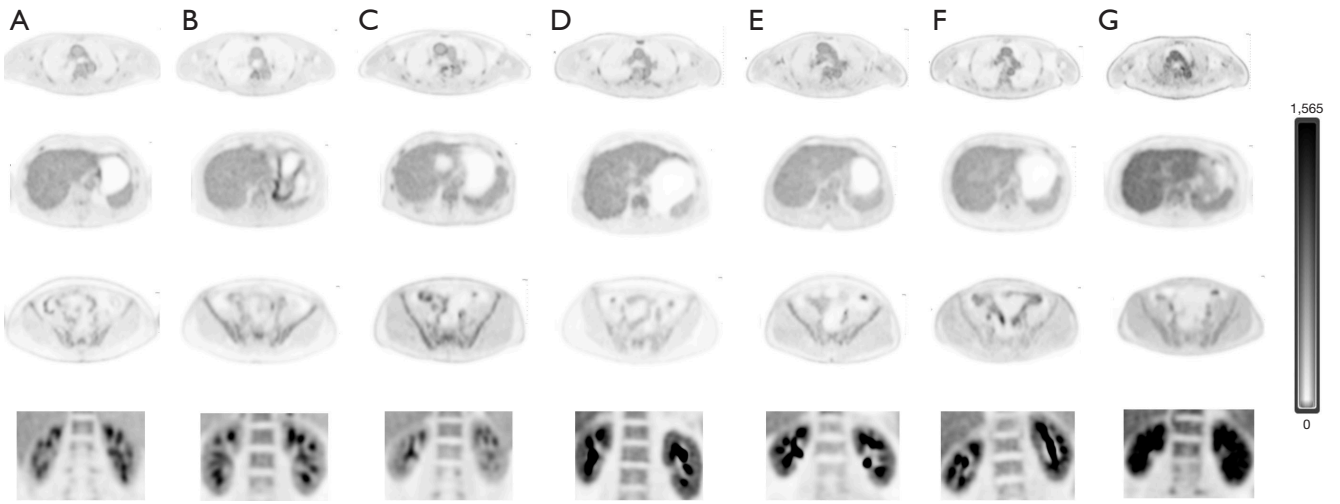

Figure 6 Tomographic images of ^{18}F-fluorodeoxyglucose positron emission tomography with different hydration protocols. (A) G1: a 49-year-old male with colorectal cancer. (B) G2: a 64-year-old male with vocal cord cancer. (C) G3: a 61-year-old male with lung cancer. (D) G4: a 64-year-old male with colorectal cancer. (E) G5: a 52-year-old male with lung cancer. (F) G6: a 70-year-old male with lung cancer. (G) Nonhydration group: a 28-year-old healthy male.

SUVmax (0.81±0.15) and SUVmean (0.62±0.13) of the muscle in the nonhydration group were significantly higher than in G1, G2, G3, and G4. However, there was no difference in muscle SUVmax and SUVmean between the nonhydration group, G5, and G6. The nonhydration control group showed a higher liver SUVmax (3.03±0.42), SUVmean (2.73±0.37), and SD (0.14±0.03) compared to the 6 hydration groups ($P<0.05$ for all hydration groups *vs.* nonhydration group), but there was no difference in the liver SNR between the nonhydration (19.79±2.72) and hydration groups. The SUVmax of the renal parenchymal (3.54±0.41) and bladder cavity [median (interquartile range): 231.4 (85.63, 377.10)] in the nonhydration group was significantly higher than in any of the 6 groups ($P<0.05$ for all hydration groups *vs.* nonhydration group).

Typical images obtained under different hydration protocols are shown in *Figures 6*,7.

Discussion

^{18}F-FDG is injected intravenously into the blood circulation and exhibits higher uptake in the tumor tissue, but this depends on the biological characteristics, while there may be a degree of distribution in normal tissues (23). The difference in the degree of uptake of ^{18}F-FDG between the tumor and the surrounding normal tissue in PET-CT imaging is important evidence for the diagnosis of disease (24). FDG is excreted by the kidneys into the urine and clearance of ^{18}F-FDG can be affected by hydration (25). Adequate hydration can increase blood capacity and help accelerate the excretion of ^{18}F-FDG, thus having a potential benefit of reducing background radioactivity (26-28). Therefore, during ^{18}F-FDG PET-CT imaging, it is important for patients to be sufficiently hydrated to improve the contrast between the tumor and normal tissue, as well as to keep patient radiation exposure levels as low as reasonably possible (7,29). To our knowledge, there are no data concerning the effects of hydration volume and time on the quantification of healthy tissue uptake in the administration of ^{18}F-FDG total-body PET-CT with half-dose activity.

The SUV is the most common parameter for quantifying the accumulation of ^{18}F-FDG in tissues in conventional PET-CT examinations (30). Partial-volume effects, the time of ^{18}F-FDG uptake, participants' preparation, and the blood glucose level all impact SUV assessment (31). Therefore, to minimize the interference elements that impact the SUV as much as possible in the present study, the interval time of all patients from the injection of ^{18}F-FDG to image acquisition of all patients was acceptable, and the difference between groups was not statistically significant. We only selected patients who did not drink water during the 6-h fasting time. Blood glucose was also strictly controlled at a level below 7.8 mmol/L. There were no statistical differences

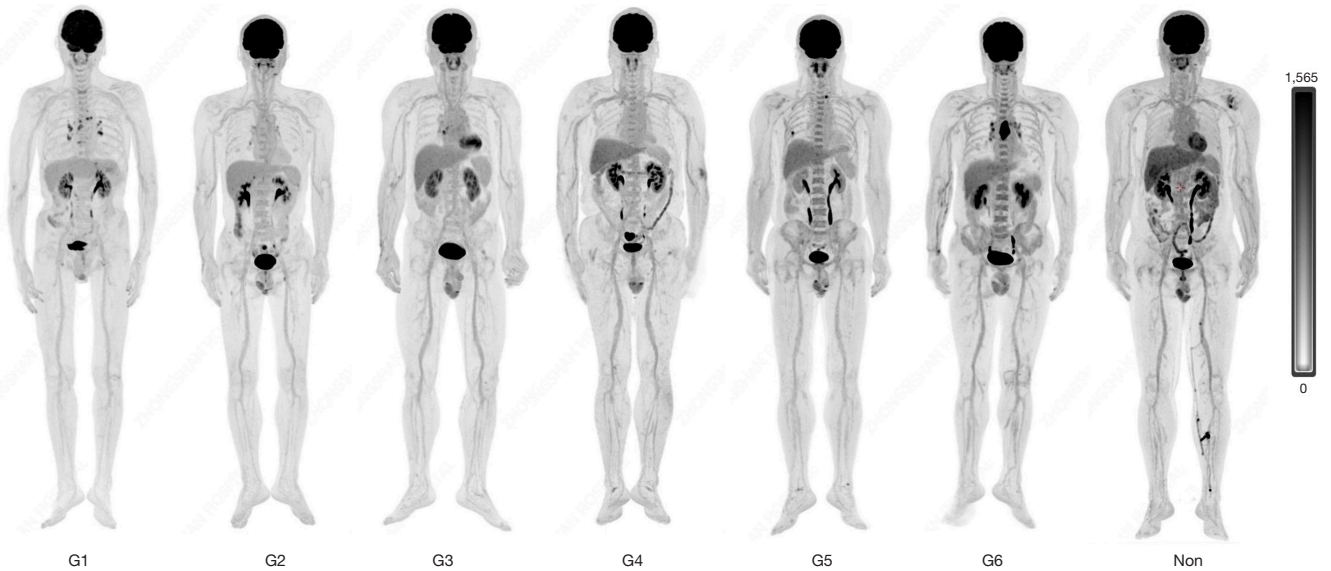

Figure 7 MIP images of ^{18}F-fluorodeoxyglucose total-body positron emission tomography with different hydration protocols. G1: a 73-year-old male with gastric cancer. G2: a 67-year-old male with colorectal cancer. G3: a 61-year-old male with lung cancer. G4: a 64-year-old male with colorectal cancer. G5: a 52-year-old male with lung cancer. G6: a 63-year-old male with esophageal cancer. Nonhydration group: a 61-year-old male with liver cancer. MIP, maximum-intensity projection.

in sex, age, weight, height, BMI, injected dose, or blood glucose level between the groups.

Different mechanisms of uptake and excretion, including the physiological activity of the normal soft tissues and the kidneys as well as the size of the tumor tissue and the metabolic activity of the malignant cells, contribute to the remaining ^{18}F-FDG concentration in the blood pool (32). Therefore, we only enrolled patients with normal renal function and no urinary tract obstruction and excluded those with excessive tumor load or high bone marrow uptake.

Our results showed that the SUV of the blood pool was related to the volume of drinking water and was related to hydration time when hydration was adequate (500 mL). With the delay in hydration time or with a decrease in the hydration volume, the quantification of the blood pool increased. Additionally, compared to the participants who did not drink any water during the fasting and uptake times, those in the hydration groups had a significantly lower SUV of the blood pool. The improved background with adequate (500 mL) hydration could be explained by the better excretion of the tracers from the kidneys, as shown by the lower SUVmax in the renal parenchyma and bladder cavity. This result suggests that adequate water intake (500 mL) 20 min before the injection of ^{18}F-FDG can significantly reduce the background radioactivity in the blood pool.

The muscle showed higher SUVmax with the delay in hydration time, but this was independent of the volume of water. Moreover, the data of the nonhydration control group indicated that compared with participants in the 20 min-before and 5 min-after groups who drank either 500 or 200 mL of water, those in the non-hydration control group had increased ^{18}F-FDG accumulation in muscular tissue, suggesting that 200 mL of water was as effective as 500 mL. This finding supports the findings of Ceriani *et al.* (32), in which compared to 500, 250 mL of liquid was found to be sufficient for reducing background activity in muscular tissue. However, Ceriani *et al.* stated that the timing of hydration is not crucial, but our study's findings suggest that drinking water 20 min before or 5 min after ^{18}F-FDG injection would be more effective.

In our study, the SUVmax, SUVmean, and SD of the liver in the nonhydration group were dramatically higher than in any of the 6 hydration groups regardless of the volume and time. However, the SNR of the liver, which was obtained by dividing the liver SUVmean in the ROI by its SD, was almost equivalent between the nonhydration group and any of the 6 hydration groups. However, there was no statistically significant difference in the effects of different hydration protocols on the liver between the groups. The liver contains high levels of metabolically active enzymes

including glucose-6-phosphatase. This enzymatic activity could further reduce the normal "metabolic trapping" of FDG-6-phosphate and overall normal liver background activity (33,34). Therefore, 200 mL of liquid may be sufficient for reducing the background activity in the liver, but the timing of hydration may be irrelevant.

This study has some potential limitations. The location of the primary lesion, tumor stage, and histologic tumor type were not comparable between the 7 groups, and thus the SUVmax of the primary lesions also varied across groups. Thus, the target–to–background ratio of the patients could not be analyzed. In addition, we used dynamic PET images reconstructed from the last 10 min of data to simulate static acquisition scenarios. Although participants who underwent static PET-CT were required to rest quietly for about 60 min after the injection of ^{18}F-FDG, physical activities such as movement from the waiting room to the restroom and examination room were unavoidable. However, the 75- or 60-min dynamic PET acquisition was started with the bolus injection of ^{18}F-FDG throughout which participants lay on the examination bed. The patient's physical activity might have influenced the distribution of ^{18}F-FDG. Previously, our team explored the feasibility of reduced injected activity and shorter PET acquisition duration (14,15). Total-body PET-CT with half-dose activity and a 10-min acquisition time is one of the routine protocols in our department (35,36). Therefore, this study only examined hydration in patients who underwent half-dose PET-CT imaging. There is still a lack of understanding concerning how hydration affects the quantification of healthy tissue uptake with full or ultralow doses. Finally, no dosimetry information was provided in this study.

Conclusions

When total-body PET-CT with a half dose of ^{18}F-FDG activity is performed, hydration can significantly affect the quantification of healthy tissue uptake. With adequate (500 mL) water intake, drinking water 20 min before injection showed lower quantification of blood pool uptake compared to drinking water 5 or 30 min after injection. Drinking 500 or 200 mL water 20 min before or 5 min after injection can significantly reduce the quantification of muscle uptake.

Acknowledgments

We would like to thank Editage (www.editage.cn) for English language editing.

Funding: This study was funded by the Shanghai Municipal Key Clinical Specialty Project (No. SHSLCZDZK03401 to H Shi), the Three-year Action Plan of Clinical Skills and Innovation of Shanghai Hospital Development Center (No. SHDC2020CR3079B to H Shi), the Next Generation Information Infrastructure Construction Project Founded by the Shanghai Municipal Commission of Economy and Informatization (No. 201901014 to H Shi), and the Science and Technology Committee of Shanghai Municipality (No. 20DZ2201800 to Y Zhang).

Footnote

Conflicts of Interest: All authors have completed the ICMJE uniform disclosure form (available at https://qims.amegroups.com/article/view/10.21037/qims-22-440/coif). HS reports that this study was funded by the Shanghai Municipal Key Clinical Specialty Project (No. SHSLCZDZK03401), the Three-year Action Plan of Clinical Skills and Innovation of Shanghai Hospital Development Center (No. SHDC2020CR3079B), and the Next Generation Information Infrastructure Construction Project Founded by the Shanghai Municipal Commission of Economy and Informatization (No. 201901014). YZ reports that this study was funded by the Science and Technology Committee of Shanghai Municipality (No. 20DZ2201800). The other authors have no conflicts of interest to declare.

Ethical Statement: The authors are accountable for all aspects of the work in ensuring that questions related to the accuracy or integrity of any part of the work are appropriately investigated and resolved. This study was conducted in accordance with the Declaration of Helsinki (as revised in 2013) and approved by the Ethics Committee of Zhongshan Hospital, Fudan University (No. B2019-160R) Written informed consent was obtained from all enrolled patients.

References

1. Bosch KD, Chicklore S, Cook GJ, Davies AR, Kelly M, Gossage JA, Baker CR. Staging FDG PET-CT changes management in patients with gastric adenocarcinoma who are eligible for radical treatment. Eur J Nucl Med Mol Imaging 2020;47:759-67.
2. Kang F, Mu W, Gong J, Wang S, Li G, Li G, Qin W, Tian J, Wang J. Integrating manual diagnosis into radiomics for reducing the false positive rate of (18)F-FDG PET/CT diagnosis in patients with suspected lung cancer. Eur J Nucl Med Mol Imaging 2019;46:2770-9.
3. Wang H, Zhao S, Li L, Tian R. Development and validation of an (18)F-FDG PET radiomic model for prognosis prediction in patients with nasal-type extranodal natural killer/T cell lymphoma. Eur Radiol 2020;30:5578-87.
4. Adili D, Cai D, Wu B, Yu H, Gu Y, Zhang Y, Shi H. An exploration of the feasibility and clinical value of half-dose 5-h total-body (18)F-FDG PET/CT scan in patients with Takayasu arteritis. Eur J Nucl Med Mol Imaging 2023;50:2375-85.
5. Marcucci F, Rumio C. On the Role of Glycolysis in Early Tumorigenesis-Permissive and Executioner Effects. Cells 2023;12:1124.
6. Shirakawa K, Sano M. Sodium-Glucose Co-Transporter 2 Inhibitors Correct Metabolic Maladaptation of Proximal Tubular Epithelial Cells in High-Glucose Conditions. Int J Mol Sci 2020;21:7676.
7. Boellaard R, Delgado-Bolton R, Oyen WJ, Giammarile F, Tatsch K, Eschner W, et al. FDG PET/CT: EANM procedure guidelines for tumour imaging: version 2.0. Eur J Nucl Med Mol Imaging 2015;42:328-54.
8. Shankar LK, Hoffman JM, Bacharach S, Graham MM, Karp J, Lammertsma AA, Larson S, Mankoff DA, Siegel BA, Van den Abbeele A, Yap J, Sullivan D; National Cancer Institute. Consensus recommendations for the use of 18F-FDG PET as an indicator of therapeutic response in patients in National Cancer Institute Trials. J Nucl Med 2006;47:1059-66.
9. Delbeke D, Coleman RE, Guiberteau MJ, Brown ML, Royal HD, Siegel BA, Townsend DW, Berland LL, Parker JA, Hubner K, Stabin MG, Zubal G, Kachelriess M, Cronin V, Holbrook S. Procedure guideline for tumor imaging with 18F-FDG PET/CT 1.0. J Nucl Med 2006;47:885-95.
10. Badawi RD, Shi H, Hu P, Chen S, Xu T, Price PM, Ding Y, Spencer BA, Nardo L, Liu W, Bao J, Jones T, Li H, Cherry SR. First Human Imaging Studies with the EXPLORER Total-Body PET Scanner. J Nucl Med 2019;60:299-303.
11. Cherry SR, Jones T, Karp JS, Qi J, Moses WW, Badawi RD. Total-Body PET: Maximizing Sensitivity to Create New Opportunities for Clinical Research and Patient Care. J Nucl Med 2018;59:3-12.
12. Zhang X, Xie Z, Berg E, Judenhofer MS, Liu W, Xu T, et al. Total-Body Dynamic Reconstruction and Parametric Imaging on the uEXPLORER. J Nucl Med 2020;61:285-91.
13. Tan H, Sui X, Yin H, Yu H, Gu Y, Chen S, Hu P, Mao W, Shi H. Total-body PET/CT using half-dose FDG and compared with conventional PET/CT using full-dose FDG in lung cancer. Eur J Nucl Med Mol Imaging 2021;48:1966-75.
14. Zhang YQ, Hu PC, Wu RZ, Gu YS, Chen SG, Yu HJ, Wang XQ, Song J, Shi HC. The image quality, lesion detectability, and acquisition time of (18)F-FDG total-body PET/CT in oncological patients. Eur J Nucl Med Mol Imaging 2020;47:2507-15.
15. Liu G, Yu H, Shi D, Hu P, Hu Y, Tan H, Zhang Y, Yin H, Shi H. Short-time total-body dynamic PET imaging performance in quantifying the kinetic metrics of (18) F-FDG in healthy volunteers. Eur J Nucl Med Mol Imaging 2022;49:2493-503.
16. Hu Y, Liu G, Yu H, Gu J, Shi H. Diagnostic performance of total-body (18)F-FDG PET/CT with fast 2-min acquisition for liver tumours: comparison with conventional PET/CT. Eur J Nucl Med Mol Imaging 2022;49:3538-46.
17. Liu G, Hu P, Yu H, Tan H, Zhang Y, Yin H, Hu Y, Gu J, Shi H. Ultra-low-activity total-body dynamic PET imaging allows equal performance to full-activity PET imaging for investigating kinetic metrics of (18)F-FDG in healthy volunteers. Eur J Nucl Med Mol Imaging 2021;48:2373-83.
18. Hu Y, Liu G, Yu H, Wang Y, Li C, Tan H, Chen S, Gu J, Shi H. Feasibility of Acquisitions Using Total-Body PET/CT with an Ultra-Low (18)F-FDG Activity. J Nucl Med 2022;63:959-65.
19. Tan H, Gu Y, Yu H, Hu P, Zhang Y, Mao W, Shi H. Total-Body PET/CT: Current Applications and Future Perspectives. AJR Am J Roentgenol 2020;215:325-37.
20. Spencer BA, Berg E, Schmall JP, Omidvari N, Leung EK, Abdelhafez YG, Tang S, Deng Z, Dong Y, Lv Y, Bao J, Liu

W, Li H, Jones T, Badawi RD, Cherry SR. Performance Evaluation of the uEXPLORER Total-Body PET/CT Scanner Based on NEMA NU 2-2018 with Additional Tests to Characterize PET Scanners with a Long Axial Field of View. J Nucl Med 2021;62:861-70.
21. Vandenberghe S, Moskal P, Karp JS. State of the art in total body PET. EJNMMI Phys 2020;7:35.
22. de Groot EH, Post N, Boellaard R, Wagenaar NR, Willemsen AT, van Dalen JA. Optimized dose regimen for whole-body FDG-PET imaging. EJNMMI Res 2013;3:63.
23. Caracó C, Aloj L, Chen LY, Chou JY, Eckelman WC. Cellular release of 18F2-fluoro-2-deoxyglucose as a function of the glucose-6-phosphatase enzyme system. J Biol Chem 2000;275:18489-94.
24. Chin BB, Green ED, Turkington TG, Hawk TC, Coleman RE. Increasing uptake time in FDG-PET: standardized uptake values in normal tissues at 1 versus 3 h. Mol Imaging Biol 2009;11:118-22.
25. Miller JH, Mullin JM, McAvoy E, Kleinzeller A. Polarity of transport of 2-deoxy-D-glucose and D-glucose by cultured renal epithelia (LLC-PK1). Biochim Biophys Acta 1992;1110:209-17.
26. Akers SR, Werner TJ, Rubello D, Alavi A, Cheng G. 18F-FDG uptake and clearance in patients with compromised renal function. Nucl Med Commun 2016;37:825-32.
27. Higashiyama A, Komori T, Juri H, Inada Y, Azuma H, Narumi Y. Detectability of residual invasive bladder cancer in delayed (18)F-FDG PET imaging with oral hydration using 500 mL of water and voiding-refilling. Ann Nucl Med 2018;32:561-7.
28. Cussó L, Desco M. Suppression of 18F-FDG signal in the bladder on small animal PET-CT. PLoS One 2018;13:e0205610.
29. Pace L, Nicolai E, Luongo A, Aiello M, Catalano OA, Soricelli A, Salvatore M. Comparison of whole-body PET/CT and PET/MRI in breast cancer patients: lesion detection and quantitation of 18F-deoxyglucose uptake in lesions and in normal organ tissues. Eur J Radiol 2014;83:289-96.
30. Keramida G, Peters AM. The appropriate whole body metric for calculating standardised uptake value and the influence of sex. Nucl Med Commun 2019;40:3-7.
31. Adams MC, Turkington TG, Wilson JM, Wong TZ. A systematic review of the factors affecting accuracy of SUV measurements. AJR Am J Roentgenol 2010;195:310-20.
32. Ceriani L, Suriano S, Ruberto T, Giovanella L. Could different hydration protocols affect the quality of 18F-FDG PET/CT images? J Nucl Med Technol 2011;39:77-82.
33. Keiding S. Bringing physiology into PET of the liver. J Nucl Med 2012;53:425-33.
34. Mahmud MH, Nordin AJ, Ahmad Saad FF, Azman AZ. Impacts of biological and procedural factors on semiquantification uptake value of liver in fluorine-18 fluorodeoxyglucose positron emission tomography/computed tomography imaging. Quant Imaging Med Surg 2015;5:700-7.
35. Sui X, Liu G, Hu P, Chen S, Yu H, Wang Y, Shi H. Total-Body PET/Computed Tomography Highlights in Clinical Practice: Experiences from Zhongshan Hospital, Fudan University. PET Clin 2021;16:9-14.
36. Yu H, Gu Y, Fan W, Gao Y, Wang M, Zhu X, Wu Z, Liu J, Li B, Wu H, Cheng Z, Wang S, Zhang Y, Xu B, Li S, Shi H. Expert consensus on oncological [18F]FDG total-body PET/CT imaging (version 1). Eur Radiol 2023;33:615-26.

Cite this article as: Cao Y, Cai D, Sui X, Wang X, Song J, Tan H, Hu P, Zhang Y, Yu H, Shi H. Different hydration protocols for the quantification of healthy tissue uptake of half-dose ^{18}F-FDG total-body positron emission tomography–computed tomography: a prospective study. Quant Imaging Med Surg 2023;13(9):5701-5712. doi: 10.21037/qims-22-440

